ELSEVIER

Journal of Molecular Catalysis A: Chemical 163 (2000) 233–250

JOURNAL OF MOLECULAR CATALYSIS A: CHEMICAL

www.elsevier.com/locate/molcata

Influence of metal–support interactions on the kinetics of liquid-phase citral hydrogenation

Utpal K. Singh, M. Albert Vannice*

Department of Chemical Engineering, The Pennsylvania State University, University Park, PA 16802, USA

Received 2 February 2000; accepted 1 April 2000

Abstract

The kinetics of liquid-phase hydrogenation of citral (3,7-dimethyl-2,6-octadienal) on Pt/TiO_2 catalysts were studied between 298–423 K and 7–21 atm H_2 and compared to those reported earlier for Pt/SiO_2 catalysts. The kinetic data were shown to be free of transport limitations by application of the Madon–Boudart test and the Weisz–Prater criterion. Near zero- and first-order kinetics were observed for the initial rate of citral hydrogenation over the Pt/TiO_2-LTR ($T_{red} = 473$ K) and Pt/SiO_2 catalysts with respect to citral concentration and hydrogen pressure, respectively. In contrast, each dependency dropped by about one order with Pt/TiO_2-HTR ($T_{red} = 773$ K) catalysts as they were negative first-order on citral concentration and near zero-order on hydrogen pressure. Furthermore, the initial rates over Pt/TiO_2-LTR and Pt/SiO_2 exhibited an activity minimum as temperature increased whereas conventional Arrhenius behavior was exhibited by Pt/TiO_2-HTR with an activation energy of 18 kcal/mol. Pt/TiO_2-LTR and HTR catalysts initially exhibited 90% selectivity to the unsaturated alcohol as compared to 40% for hydrogenation over Pt/SiO_2. Metal–support interactions (MSI) resulted in a dramatic enhancement in specific activity at 373 K, 20 atm H_2 and 1 M citral in hexane as Pt/TiO_2-HTR exhibited a turnover frequency of 1.0 compared to 0.02 s^{-1} for Pt/TiO_2-LTR and 0.004 s^{-1} for Pt/SiO_2. The reaction kinetics with Pt/TiO_2-HTR in the differential conversion regime were described by a conventional Langmuir–Hinshelwood model assuming quasi-equilibrium for reactant adsorption, competitive adsorption between citral and hydrogen, and addition of the first H atom as the rate determining step. The reaction rate at higher conversions was modeled by invoking a decarbonylation reaction similar to that proposed earlier for this reaction over Pt/SiO_2 catalysts to explain any observed deactivation.

Keywords: Citral hydrogenation; Metal–support interactions; Pt/Tio_2-LTR; Zero-order kinetics

1. Introduction

The motivation for studying the hydrogenation of α,β-unsaturated aldehydes has been addressed by previous researchers [1,2]. These aldehydes and their hydrogenated products are important intermediates for production of perfumes, fragrances, and pharmaceuticals [3]. Considerable effort has been devoted towards studying such reactions in the vapor phase, with a particular emphasis towards obtaining mechanistic information [2,4–7], whereas most of the liquid-phase work has focused on selectivity issues in regards to enhancing the production of unsaturated alcohols [8,9]. Consequently, a number of issues remain to be addressed regarding liquid-phase hydrogenation reactions, including effect of reaction parameters and metal–support interactions [1].

Since the initial publication of Tauster et al. [10], significant effort has been devoted to a better understanding of MSI and its influence on the chemistry

* Corresponding author. Tel.: +1-814-863-4803; fax: +1-814-865-7846.
E-mail address: mavche@engr.psu.edu (M.A. Vannice).

1381-1169/00/$ – see front matter
PII: S1381-1169(00)00389-7

of different reactions, particularly hydrogenation of the C=O moiety [10–14]. MSI with titania-supported Group VIII metals is induced by reduction at high temperatures, i.e. 773 K, which results in formation of oxygen vacancies in the form of coordinatively unsaturated cations at the metal–support interface, migration of the partially reduced support, TiO_x ($x < 2$), onto the metal, and suppression of H_2 and CO chemisorption by site blockage [15]. Sen and Vannice have previously shown that MSI can be used to favor the vapor-phase hydrogenation of the C=O bond in acetone and crotonaldehyde over Pt/TiO_2-HTR (high temperature reduced) catalysts [5,16]. Activation of the C=O bond in the vapor-phase reaction on Group VIII metals supported on reducible supports has received much attention [5,6,11,13,14,16,17] however, much less work has been conducted on liquid-phase reactions, and most of that has focused on selectivity issues related to catalyst characterization [18–21]. There is a dearth of quantitative studies regarding the influence of MSI on the kinetics of liquid-phase reactions.

In the present paper, we have examined the influence of MSI on a liquid-phase hydrogenation reaction over Pt/TiO_2 catalysts. The kinetic data were free of mass transfer limitations, as verified by the Madon–Boudart test and the Weisz–Prater criterion [22,23], and an emphasis was placed on obtaining reliable kinetics in the differential reaction regime (citral conversion < 20%). Extra precautions were taken to ensure dry and anaerobic conditions throughout the reaction. This is particularly important for catalysts in the MSI (or SMSI, i.e. strong metal–support interactions as it is sometimes referred to) state since it has been shown that exposure to air or O_2 at room temperature is sufficient to remove SMSI behavior with Rh/TiO_2 catalysts [24]. Although Pt/TiO_2-HTR catalysts require higher exposure temperatures to reverse the SMSI effect, this complication was avoided by utilizing anaerobic conditions [24].

2. Experimental

2.1. Catalyst preparation and characterization

TiO_2 (Degussa P25-50 m^2/g, 20% rutile, 80% anatase, 60–100 mesh) was dried and calcined at 773 K for 4 h prior to impregnation. Catalysts were prepared with hydrogen hexachloroplatinate (IV) hydrate (H_2PtCl_6-Aldrich 99.995%) using the incipient wetness technique, i.e. an aqueous solution of chloroplatinic acid was added dropwise to a calcined support to fill the pore volume (1.0 cm^3/g TiO_2, 2.2 cm^3/g SiO_2) and subsequently dried at 393 K overnight. Hydrogen chemisorption was measured at 300 K after reduction in a static volumetric apparatus with a base pressure of 10^{-7} Torr using a procedure described elsewhere [25]. Although dual isotherms were obtained, Pt dispersions were calculated using the value of the total H_2 uptake isotherm extrapolated to zero pressure and assuming an adsorption stoichiometry of unity, i.e. H_{ad}:Pt_s ratio of 1.

2.2. Catalytic hydrogenation

Hydrogenation experiments were conducted in a 100 ml EZ-seal autoclave with an automated data acquisition system to monitor H_2 uptakes. Details have been provided elsewhere [26,27]. The reactor was loaded with 0.5 g of catalyst, sealed, and leak tested at 54 atm to ensure a tight seal. Helium (MG Industries 99.99%) was used as received while H_2 (MG Industries 99.99%) was further purified by passage through a high pressure moisture trap (Alltech) and an Oxytrap (Alltech). Five pressure/vent cycles were conducted at 300 K by pressurizing the reactor to 54 atm in He then venting to atmospheric pressure to remove all traces of oxygen from inside the reactor. The pretreatment procedure was initiated by flowing 200 cm^3(STP) He/min through the reactor while heating it at 120 K/h from room temperature to the desired reduction temperature. The flow was then switched to 500 cm^3(STP)/min H_2 for 75 min prior to cooling to room temperature and storing overnight under a static atmosphere of 1.4 atm H_2. Pt/SiO_2, Pt/TiO_2-LTR, and Pt/TiO_2-HTR catalysts were reduced at 673, 473, and 773 K, respectively. This storage procedure had no effect on catalytic behavior as evidenced by identical turnover frequencies (TOFs) and product distributions, within experimental uncertainty, after either storage overnight or use immediately after the reduction.

The standard reaction conditions were 20 atm hydrogen pressure and 1 mol citral/l hexane with a total reaction volume of 60 ml. Citral and hexane were degassed by sparging for 30 min with high flow rates of nitrogen (99.99% MG), which was further purified

by passage through a hydrocarbon and moisture trap (Alltech Assoc.), for 30 min prior to injection into the reactor. Hexane (Fisher 99.90% saturated C_6 hydrocarbons) was pumped into the reactor at reaction temperature and pressure using a high pressure syringe pump (ISCO 500D) in a closed system to prevent any exposure to air. The hexane/catalyst slurry was stirred at 1000 rpm and allowed to equilibrate for 30 min prior to the introduction of citral. The pressure was continuously maintained to within 5% of the set point with a Brooks 5860 pressure controller during these semi-batch reactor experiments, and the pressure decay within this 5% range (19–21 atm, for example) was monitored to obtain the instantaneous rate of H_2 uptake at any time during the reaction. In addition, liquid samples (0.5 ml) were periodically withdrawn through a dip tube extending inside the reactor, collected in a closed, N_2-purged vessel, and analyzed in a H-P 5890 gas chromatograph equipped with a thermal conductivity detector and a six feet Carbowax 20 M (10% on Supelcoport) packed column. Initial rates of citral disappearance were evaluated using the slope of the linear portion of the temporal citral conversion profile (for citral conversions less than 20%). The cumulative product selectivity was calculated as follows:

$$S_i = \frac{\text{concentration of species } i}{\sum_{\text{products}} \text{concentration of species } i} \quad (1)$$

3. Results

Citral hydrogenation presents a complex reaction network [27], but reaction over Pt/TiO_2 catalysts strongly favored hydrogenation of the conjugated C=C and C=O bonds, therefore, Fig. 1 displays a sufficiently descriptive reaction network for citral hydrogenation over these catalysts. Table 1 presents the hydrogen chemisorption results for Pt/SiO_2, Pt/TiO_2-LTR, and Pt/TiO_2-HTR. Reduction at 773 K resulted in a large suppression of H_2 chemisorption (ca. 90% or greater) for all the Pt/TiO_2 catalysts due to blockage of Pt adsorption sites by migration of TiO_x species, which is consistent with MSI behavior [11–15]. The Pt/TiO_2-LTR catalysts exhibited normal chemisorption behavior with dispersions near unity and concentrations of surface Pt atoms varying from 26 to 112 μmol Pt_s/g cat which represents a greater than fourfold variation. The Madon–Boudart test [22] was previously conducted with a family of Pt/SiO_2 catalysts possessing an order of magnitude variation in Pt_s concentration, but similar dispersion, to verify the absence of external and internal heat/mass transfer limitations [22]. Moreover, all reactions were conducted at 1000 rpm after previous studies showed that external mass transfer limitations disappeared at stirring rates greater than 500 rpm. The reaction was conducted at standard conditions over 0.61, 1.24, 1.78, and 1.92% Pt/TiO_2-HTR catalysts, all with

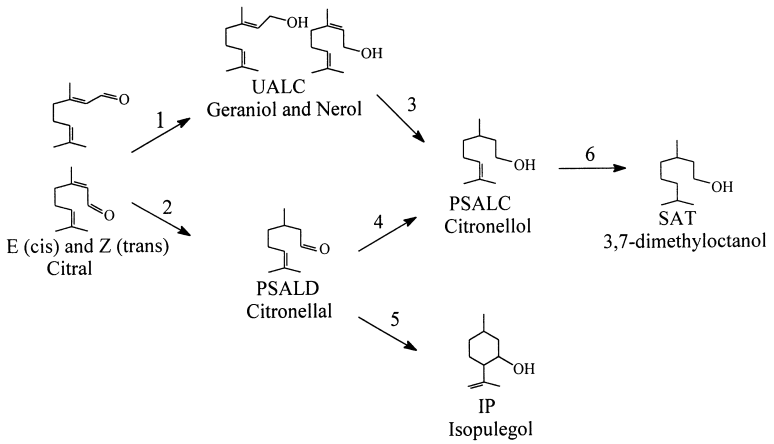

Fig. 1. Reaction network for citral hydrogenation over Pt/TiO_2 catalysts.

Table 1
H_2 chemisorption at 300 K and initial reaction rates at 373 K, 20 atm H_2 and 1 M citral in hexane

Catalyst	H_2 uptake (μmol/g cat)				Initial activity (μmol/g cat/min)	Initial TOF (s^{-1})[a]
	$(H_2)_{Total}$	$(H_2)_{Rev}$	H/Pt	d (nm)		
1.44% Pt/SiO_2	15.2	7.4	0.41	2.8	31	0.017
3.8% Pt/SiO_2	64.1	24.6	67.00	1.7	53	0.007
0.77% Pt/SiO_2	26.5	11.3	1.00	1.1	0.11	0.004
1.24% Pt/TiO_2 (LTR)	31.2	13.8	0.98	1.2	–	–
1.24%Pt/TiO_2 (HTR)	4.0	3.4	0.12		265	0.55 (0.071)
0.61% Pt/TO_2 (LTR)	13.0	6.8	0.97	1.2	39	0.025
0.61% Pt/TiO2 (HTR)	0.4	0.2	0.00	–	90	1.9 (0.058)
1.78% Pt/TiO2 (LTR)	43.6	23.3	0.96	1.2	52	0.01
1.78% Pt/TiO_2 (HTR)	2.8	1.0	0.02	–	319	0.95 (0.061)
1.92% Pt/TiO_2 (LTR)	56.1	21.4	1.00	1.1	201	0.03
1.92% Pt/TiO_2 (HTR)	2.5	1.2	0.03	336	–	1.12 (0.05)

[a] Values in parentheses represents TOF for an HTR catalyst normalized to H_2 chemisorption for an LTR catalyst.

dispersions near unity, and similar TOFs were exhibited by each of these catalysts, as shown in Table 1. Fig. 2 displays a ln–ln plot of initial activity versus Pt_s concentration for reaction at 373 K, 20 atm H_2 with 1 M citral in hexane over a family of Pt/TIO_2-LTR and HTR catalysts, which give respective slopes of 0.84 and 0.90. The near unity slopes, within experimental uncertainty, indicates the absence of mass transfer effects. The TOFs were only compared at 373 K, however, this comparison along with the Weisz–Prater criterion [23] is sufficient to demonstrate the absence of all transport limitations in these results as will be discussed later. The dimensionless Weisz–Prater parameter was evaluated for each of the catalysts at standard reaction conditions, and it was of the order of 10^{-2}, as shown in Table 2 , thus verifying that the reaction kinetics are not affected by internal diffusion resistance. Absence of transport limitations with the Pt/TiO_2-HTR catalysts guarantees that the kinetics over Pt/TiO_2-LTR catalysts are also free of transport limitations because the reaction rates over the latter catalysts are lower than those with the former.

Fig. 3 and Table 2 display the reaction orders over Pt/SiO_2, Pt/TiO_2-LTR and Pt/TiO_2-HTR catalysts in

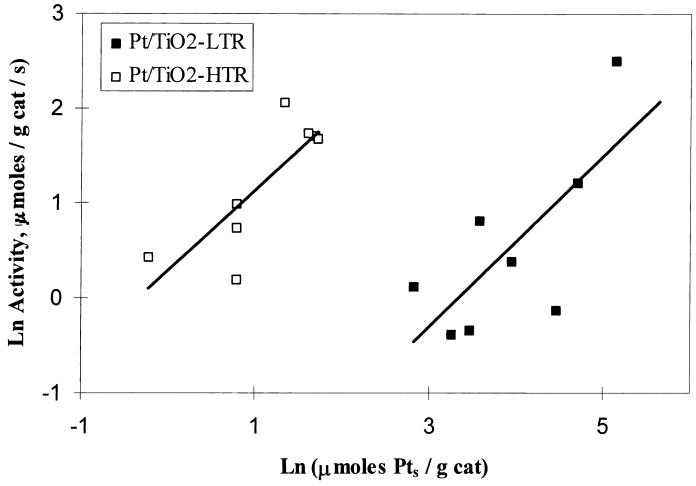

Fig. 2. Madon–Boudart test for mass transfer limitations over a family of Pt/TiO_2-LTR and HTR catalysts during reaction at 373 K, 20 atm H_2 and 1 M citral in hexane.

Table 2
Weisz–Prater parameters evaluated for reaction at 373 K, 20 atm H_2 and 1 M citral in hexane over Pt/TiO_2-HTR catalysts[a]

Catalyst Pt/TiO_2 (%)	Dimensionless Weisz–Prater parameter
0.61	0.015
1.78	0.058
1.92	0.062

[a] $D_{eff} = 16.4 \times 10^{-5}\,cm^2/s$, $C_s = 8.3 \times 10^{-6}\,mol/cm^3$, $d = 0.0055\,cm$.

the citral concentration range of 0.5–5.9 M citral and a H_2 pressure range of 7–42 atm. Pt/SiO_2 catalysts exhibited approximately zero- and first-order dependencies on citral concentration and hydrogen pressure, respectively [27]. In stark contrast, Pt/TiO_2-HTR exhibited a −0.9 dependence on citral concentration and a near zero-order dependence on hydrogen pressure. Although substantial scatter exists among Pt/TiO_2-HTR data, it must be emphasized that a fresh catalyst sample was used for each of the runs, i.e. each data point, thus increasing the uncertainty.

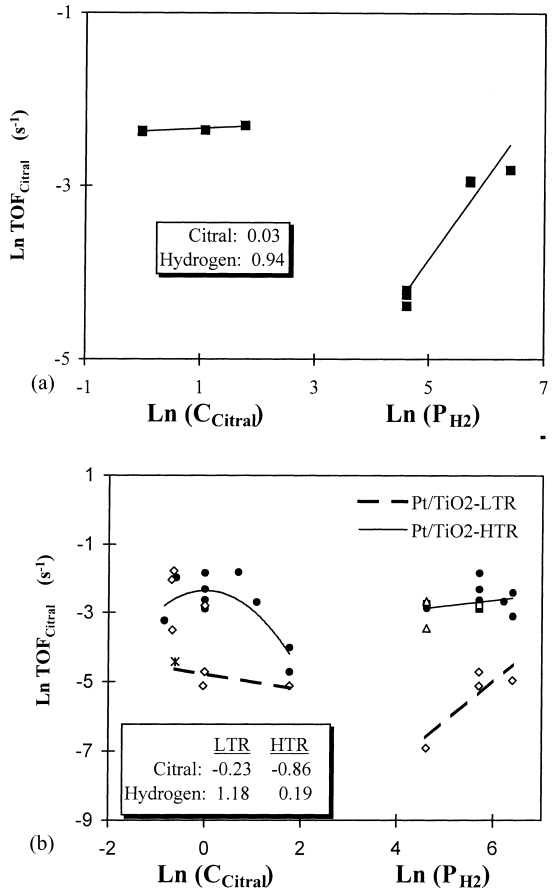

Fig. 3. Effect of citral concentration and hydrogen pressure on the initial rate of citral disappearance for reaction at 373 K, 7–41 atm H_2, and 0.5–6.0 M citral in hexane over (a) 1.44% Pt/SiO_2 catalyst, (b) ● — 0.61% Pt/TiO_2, ◇ — 1.78% Pt/TiO_2, △ — 1.24% Pt/TiO_2, ∗ — 1.92% Pt/TiO_2.

Fig. 4a and b display the temporal concentration and hydrogenation rate profiles profiles during citral hydrogenation at standard conditions over 1.78% Pt/TiO_2-HTR. The concentrations of *cis* and *trans* isomers (or *Z*- and *E*-isomers, respectively) of citral exhibit a sustained decrease with time, and the primary products observed were geraniol and nerol (unsaturated alcohols). Fig. 4b displays the hydrogenation rate during the course of the reaction, and a threefold decrease is observed in the TOF (μmol H_2/μmol Pt_s/s). The hydrogenation rates based on H_2 consumption were also evaluated from the concentration profiles assuming that only geraniol, nerol, and citronellal were formed, and these are superimposed in Fig. 4b with the rates obtained from the pressure data. Excellent agreement is observed between these two independent rate measurements which is indicative that H_2 consumption via side reactions is negligible.

Fig. 5 displays the TOF dependence for each citral isomer on its concentration over 1.78% Pt/TiO_2-HTR at 373 K and 20 atm H_2. Each reaction rate was evaluated based on the slope and average concentration between two sequential concentration data points in Fig. 4a. The *E*- and *Z*-isomers of citral exhibit near first- and near zero-order kinetics, respectively. Fig. 6a displays the concentration profiles and Fig. 6b shows the dependence of the TOF for each citral isomer on its concentration at 373 K and 20 atm H_2 over 1.78% Pt/TiO_2-LTR. The *E*- and *Z*-isomers exhibited reaction orders very similar to those for the Pt/TiO_2-HTR catalyst. Fig. 7 displays the temporal concentration profile for reaction over 1.44% Pt/SiO_2 at the standard conditions [27]. It is apparent from the figure that a linear trend line describes the monotonic decrease in the concentrations of *E* and *Z* citral indicative of zero-order kinetics for both isomers. Furthermore, the ratio of the TOF for disappearance of the *E*- to that for the *Z*-isomer was 1.5 and constant over time with Pt/SiO_2 whereas this ratio was initially almost four with a sustained decrease during the course of the reaction over the Pt/TiO_2-LTR and HTR catalysts.

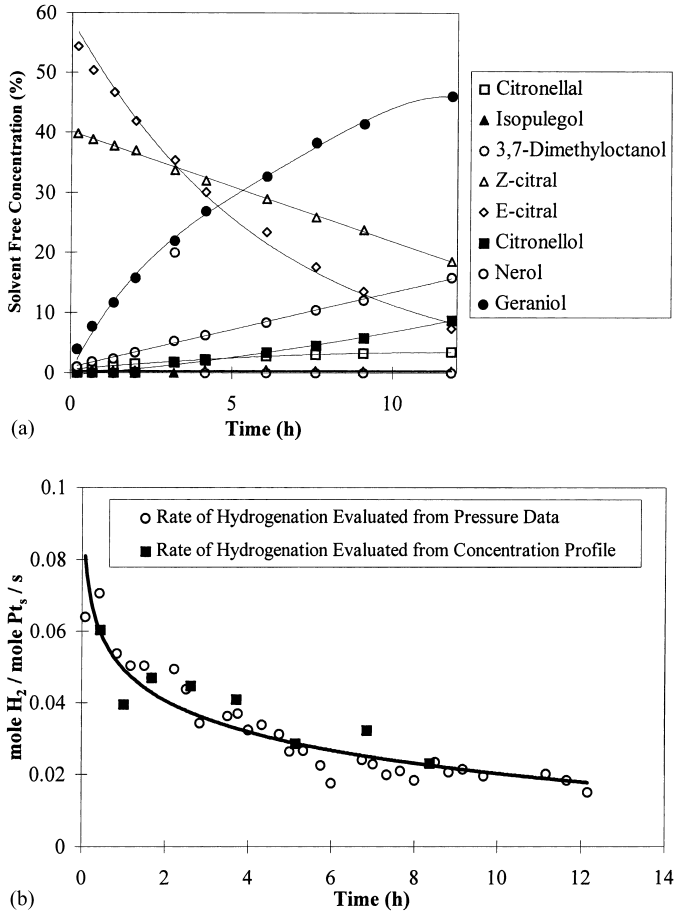

Fig. 4. (a) Temporal concentration, and (b) temporal H_2 uptake profile for citral hydrogenation over 1.78% Pt/TiO_2-HTR catalyst at 373 K, 20 atm H_2, and 1 M citral in hexane.

The zero-order kinetics with respect to the *E*- and *Z*-isomers of citral were observed with all Pt/SiO_2 catalysts independently of dispersion, temperature, and pressure, whereas the Pt/TiO_2-HTR catalysts exhibited their respective near zero- and first-order dependencies on *Z*- and *E*-isomers independently of Pt dispersion and hydrogen pressure, but the reaction was zero-order with respect to both the *E*- and *Z*-isomers of citral at 343 K and 20 atm H_2 [28].

Fig. 8 shows the TOF for H_2 consumption during citral hydrogenation on 3.8% Pt/SiO_2, 1.78% Pt/TiO_2-LTR, and 1.78% Pt/TiO_2-HTR at standard reaction conditions. Pt/TiO_2-HTR exhibits a two-order of magnitude enhancement in TOF compared to the Pt/SiO_2 catalyst with a similar Pt crystallite size, i.e. 1.7 nm for Pt/SiO_2 compared to 1 nm for Pt/TiO_2. It has been shown that HTR pretreatment does not induce any significant sintering; therefore, the Pt/TiO_2-HTR and LTR catalysts have similar Pt crystallite sizes [29]. Furthermore, the initial rate (per gram catalyst) is approximately threefold greater after a HTR step compared to a LTR step, and the TOF for Pt/TiO_2-HTR is 50-fold larger than that for Pt/TiO_2-LTR. Reaction rates with the Pt/TiO_2-LTR and HTR catalysts exhibit a markedly different dependence on temperature. Pt/TiO_2-LTR exhibits an activity minimum with increasing temperature similar to that observed with Pt/SiO_2 [27], and the results are displayed in Fig. 9a for citral hydrogenation on 1.92% Pt/TiO_2-LTR at 298, 373 and 403 K and stan-

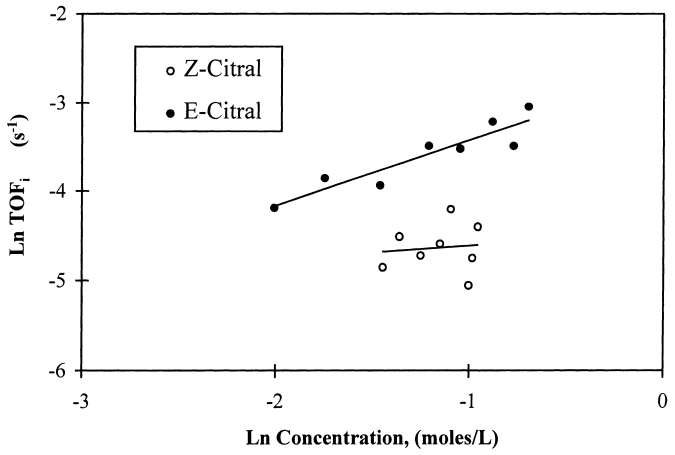

Fig. 5. Dependency of the citral isomer turnover frequency on the concentration of the respective isomer during hydrogenation over 1.78% Pt/TiO_2-HTR catalyst at 373 K, 20 atm H_2, and 1 M citral in hexane initially.

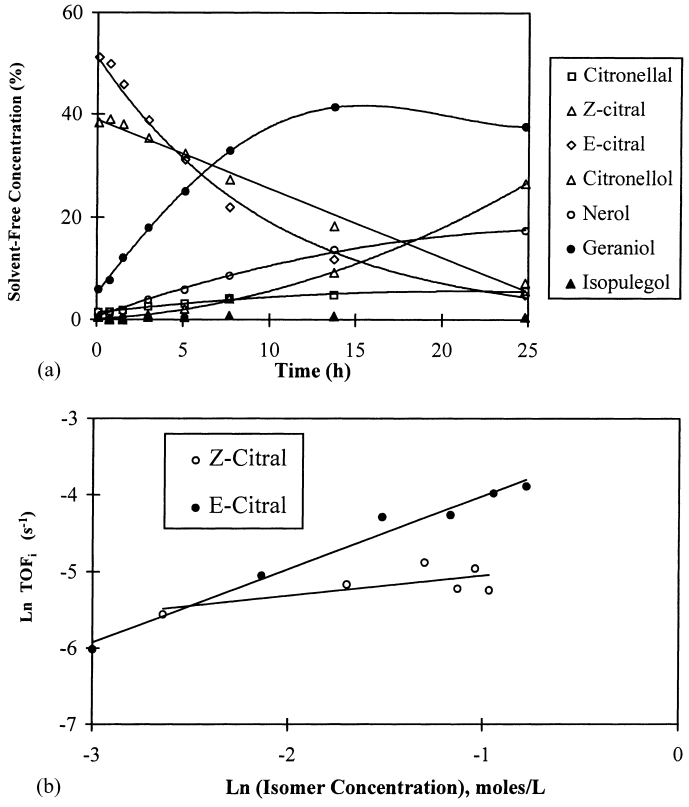

Fig. 6. (a) Temporal composition, and (b) dependence of each hydrogenation rate on the concentration of the respective isomer with 1.78% Pt/TiO_2-LTR at 373 K, 20 atm H_2, and 1 M citral in hexane, initially.

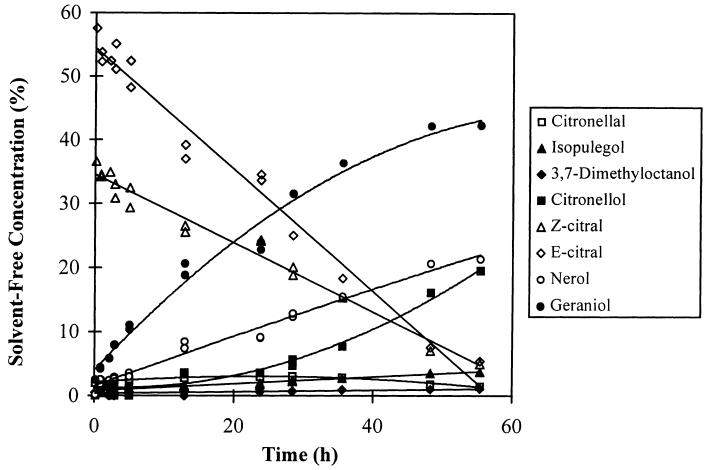

Fig. 7. Temporal concentration profile for citral hydrogenation over 1.44% Pt/SiO_2 at 373 K and 20 atm H_2 and 1 M citral in hexane, initially.

dard conditions. Substantial deactivation occurred at 298 K with the TOF for H_2 consumption decreasing from approximately 0.9 s^{-1} to negligible activity after 40% conversion. The initial TOF at 373 K was an order of magnitude lower than that at 298 K and significantly less deactivation occurred. Furthermore, the rate exhibited conventional Arrhenius behavior between 373 and 403 K with an apparent activation energy of 10 kcal/mol. In contrast, Pt/TiO_2-HTR gave normal Arrhenius behavior at all temperatures with an activation energy of 18 kcal/mol, as shown in Fig. 9b. The reaction rate on Pt/TiO_2-HTR at 298 K and standard conditions was too low to be measured accurately within a reasonable time frame; therefore only the results from 343 to 403 K are plotted in Fig. 9b.

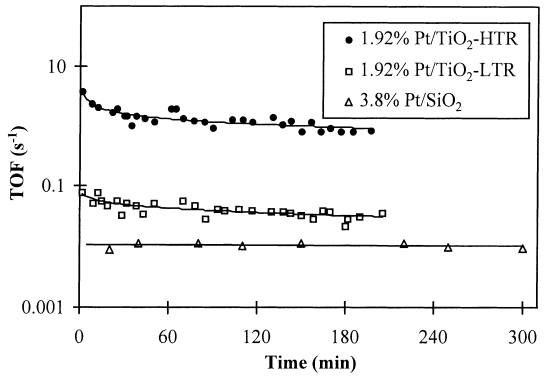

Fig. 8. Temporal rate of H_2 uptake during citral hydrogenation over 3.8% Pt/SiO_2, 1.92% Pt/TiO_2-LTR, and 1.92% Pt/TiO_2-HTR at 373 K, 20 atm H_2, and 1 M citral in hexane, initially.

Marked changes in the product distribution were observed with Pt/TiO_2 compared to Pt/SiO_2. Fig. 10 displays the selectivity to various products during reaction at standard conditions over 1.78% Pt/TiO_2-HTR. Both Pt/TiO_2-LTR and HTR catalysts exhibit similar selectivity versus conversion profile with approximately 90% selectivity to the unsaturated alcohol (geraniol + nerol) and less than 10% selectivity toward citronellol at 10% citral conversion. No 3,7-dimethyloctanol (the saturated product-SAT) was observed with either of the two catalysts. The selectivity toward citronellol, the partially saturated alcohol (PSALC), increases with increasing conversion accompanied by a slight decrease in selectivity towards the unsaturated alcohols (UALC). Fig. 11 displays a comparison of selectivity to the unsaturated alcohol versus conversion over 1.44% Pt/SiO_2, 1.78% Pt/TiO_2-LTR and HTR at standard conditions. As mentioned previously, Pt/TiO_2-LTR and Pt/TiO_2-HTR exhibit similar behavior regarding cumulative selectivity for the unsaturated alcohol versus conversion, whereas 1.44% Pt/SiO_2 exhibits an increase in selectivity from 40 initially to 80 after 50% conversion, followed by a decrease accompanied by an increase in selectivity to citronellol [30,31].

Figs. 12a and b compare the effect of temperature on the selectivity to the unsaturated alcohol (geraniol + nerol) and citronellal over 1.92%

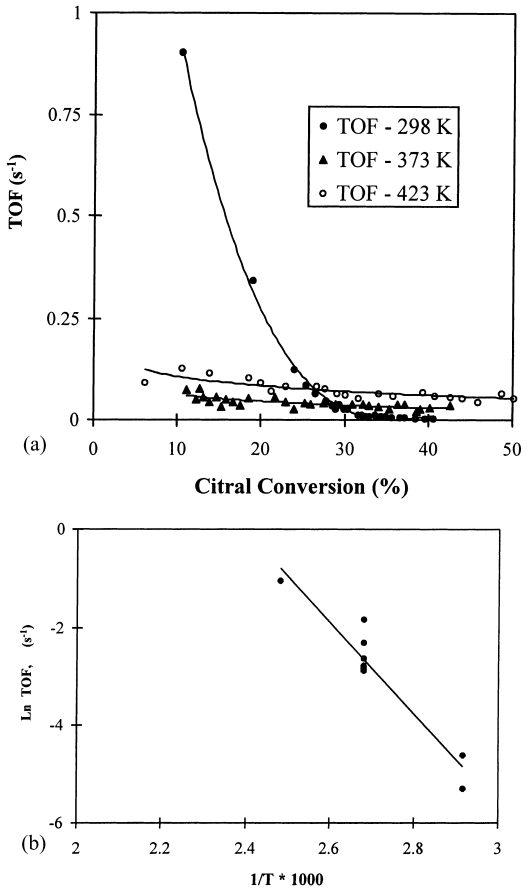

Fig. 9. (a) Temporal H_2 uptake profile for reaction over 1.92% Pt/TiO_2-LTR catalyst at 298, 373, and 403 K, 20 atm H_2, and 1 M citral in hexane, initially. (b) Arrhenius plot of the rate of initial citral disappearance over a 1.92% Pt/TiO_2-HTR catalyst in the temperature range of 343–403 K, 20 atm H_2 and 1 M citral in hexane.

Pt/TiO_2-LTR and 1.44% Pt/SiO_2 at standard conditions. Both Pt/SiO_2 and Pt/TiO_2-LTR exhibit an increase in selectivity to the unsaturated alcohol and a decrease in selectivity to citronellal as the reaction temperature increases. Furthermore, both catalysts show an increase in selectivity to UALC and a decrease in selectivity to citronellal, the partially saturated aldehyde (PSALD), with increasing citral conversion.

4. Discussion

The kinetic data reported in the present study are free of all transport limitations as verified by the Madon–Boudart test [22] and the Weisz–Prater criterion [23]. This reaction has shown little or no structure sensitivity over Pt/TiO_2 catalysts [27,31,32], which is typical for hydrogenation reactions [33]; thus the near unity slope for the plot of ln Activity versus ln Pt_s concentration in Fig. 2 indicates no significant mass transfer limitations. This is further verified by the dimensionless Weisz–Prater parameters shown in Table 2 which are of the order of 10^{-2} and below the value which assures no diffusional limitations [23]. No heat transfer limitations should be present under the reaction conditions because it has been shown that internal temperature gradients are less pronounced for liquid-solid systems compared to gas–solid systems. This is attributed to values for thermal conductivity and the product of density and heat capacity for solid–liquid systems which are about 100-fold larger than those for gas–solid systems, thus allowing more efficient heat transport from the catalyst pores [34].

Pt/TiO_2-LTR exhibits an activity minimum with respect to temperature similar to the behavior reported earlier for the hydrogenation of citral and its reaction intermediates over Pt/SiO_2 [27,33]. This temperature effect with Pt/SiO_2 was explained by postulating a concurrent side reaction involving a decomposition reaction to yield adsorbed CO and carbonaceous species. The unsaturated alcohol isomers (geraniol + nerol) were proposed to be the source of the decarbonylation reaction, however, citral could not be completely discounted [30]. Reaction over SiO_2-supported Pt at low temperatures, such as 298 K, resulted in substantial deactivation due to blockage of active sites by adsorbed CO which accumulated during the course of the reaction and eventually led to complete deactivation. At higher reaction temperatures, i.e. 373 K or above, SiO_2-supported Pt exhibited a high initial rate followed by a psuedo-steady-state rate which was an order of magnitude lower than that at 298 K. Reaction at temperatures greater than 373 K resulted in conventional Arrhenius behavior due to the enhanced rate of CO desorption [27]. This explanation, which was proposed for Pt/SiO_2 catalysts, also appears to be valid for Pt/TiO_2-LTR catalysts, which exhibit substantial deactivation of over 90% during reaction at 298 K although the initial rate at 298 K was greater than the stabilized rate observed at 373 K. An increase in temperature from 373 to 403 K resulted in conventional Arrhenius behavior.

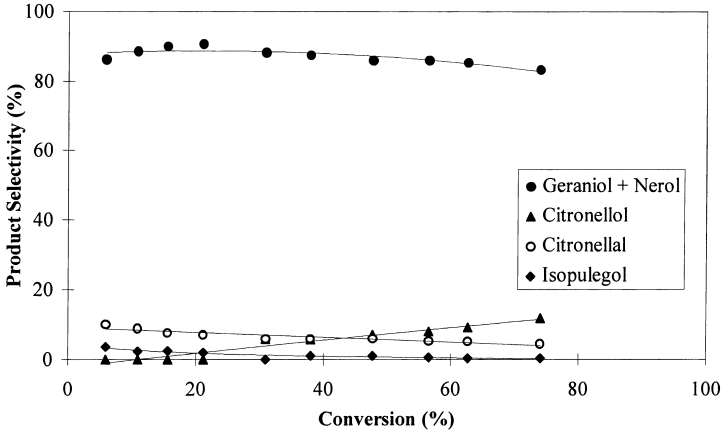

Fig. 10. Product distribution as a function of citral conversion for reaction over 1.78% Pt/TiO_2-HTR at 373 K, 20 atm H_2 and 1 M citral in hexane.

While a minimum in activity occurs with both Pt/SiO_2 and Pt/TiO_2-LTR, there are subtle differences in the kinetics between the two catalysts at 373 K that should be noted. It was previously found that reaction over Pt/SiO_2 at 373 K results in a high initial reaction rate, then deactivation and a constant lower reaction rate. The high initial reaction rate was manifested by a non-zero intercept in the temporal citral concentration profile [27]. Pt/TiO_2-LTR does not exhibit a high initial reaction rate at 373 K as is clearly indicated in Fig. 13 by the slope of the temporal profile of H_2 pressure in the reactor during the first 2 min of reaction at 373 K and standard conditions. The 1.44% Pt/SiO_2

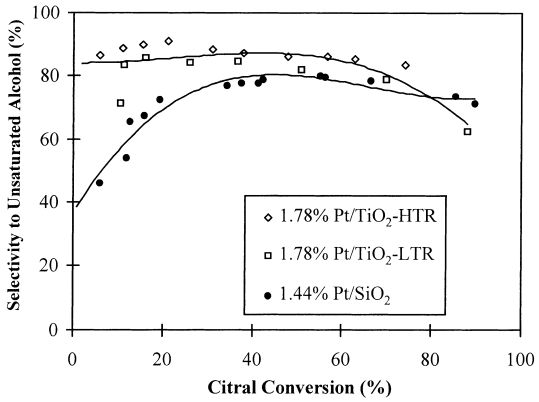

Fig. 11. Cumulative selectivity to geraniol + nerol (UALC) over 1.44% Pt/SiO_2, 1.78% Pt/TiO_2-LTR, and 1.78% Pt/TiO_2-HTR at 373 K, 20 atm H_2 and 1 M citral in hexane.

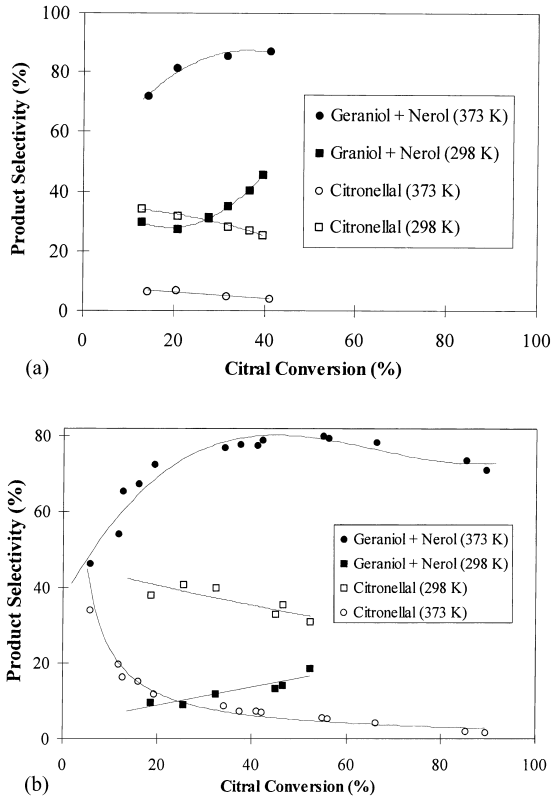

Fig. 12. Product distribution as a function of citral conversion for (a) 1.78% Pt/TiO_2-LTR, and (b) 1.44% Pt/SiO_2 at 298 K (■, □) and 373 K (○, ●), 20 atm H_2 and 1 M citral in hexane.

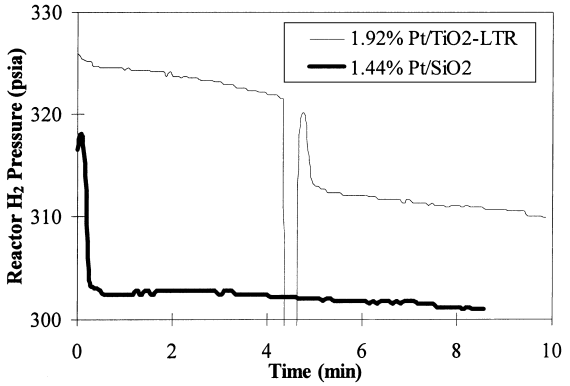

Fig. 13. Temporal reactor pressure profile during hydrogenation of 1 M citral in hexane at 373 K, 20 atm H_2 pressure over 1.44% Pt/SiO_2 and 1.92% Pt/TiO_2-LTR.

catalyst exhibited a 1.1 atm (16 psia) drop during the first minute of reaction followed by a significantly lower, but constant, rate of pressure decay, whereas Pt/TiO_2-LTR had a much lower rate of H_2 consumption during this period of time. The high initial reaction rate on Pt/SiO_2 was associated with nearly equal formation of unsaturated alcohol (UALC) and citronellal (PSALD) whereas Pt/TiO_2-LTR yielded primarily the unsaturated alcohol (see Fig. 12b). The difference in the initial product distribution between Pt/SiO_2 and Pt/TiO_2-LTR, as further indicated in Fig. 11 and Table 4, is not completely understood. It appears that even after a LTR pretreatment, MSI may influence the product distribution over Pt/TiO_2-LTR catalysts by either deactivating and/or blocking sites responsible for the rapid initial citronellal formation or by enhancing reactivity of the C=O bond. Based on past models, this would be attributed to TiO_x species on the metal or at the metal–support interface [13,14]. Reactions at 373 K and 20 atm H_2 pressure may allow a larger concentration of Ti^{3+} or Ti^{2+} species at the metal–support interface than would normally be present at atmospheric pressure [35]. Such a model could explain the absence of the crystallite size effect with Pt/TiO_2-LTR and HTR catalysts that is observed with Pt/SiO_2 catalysts containing 1–5 nm Pt crystallites [31,32].

At 373 K, the selectivity to unsaturated alcohol extrapolated to zero conversion is 90%, and it remains approximately constant with time for Pt/TiO_2-LTR and Pt/TiO_2-HTR whereas Pt/SiO_2 exhibits an initial selectivity of only 40%, but which doubles at 50% citral conversion. These selectivities, which are plotted in Figs. 10–12, are cumulative selectivity, which is an integral property, and therefore does not reflect the instantaneous changes in the product distribution during the course of the reaction. When such changes in cumulative selectivity occur with conversion, it is instructive to examine the instantaneous selectivity, which is defined as follows:

$$S_i^{\mathrm{INST}} = \frac{r_i}{\sum_{i=1}^{4} r_i} \tag{2}$$

where r_i represents the rate of reaction 1 in Fig. 1. Previous kinetic studies have shown that during citral

Table 3
Effect of metal–support interactions on the product distribution, extrapolated to zero conversion, during reaction at 373 K, 20 atm H_2, and 1 M citral in hexane

Catalyst	Geraniolt + nerol	Citronellal	Citronellol	Isopulegol	3,7-Dimethyloctanol
1.44% Pt/SiO_2	40	40	7	7	5
1.78% Pt/TiO_2-LTR	88	7	0	5	0
1.78% Pt/TiO_2-HTR	88	7	0	5	0

Table 4
Effect of metal–support interactions on the reaction orders at 373 K in the range of 1.0–6.0 M citral in hexane and 7–41 atm H_2 pressure

Catalyst	Reaction order catalyst in citral concentration	Reaction order in hydrogen pressure
1.44% Pt/SiO_2	0.03	0.9
1.78% Pt/TiO_2-LTR	−0.2	1.2
1.78% Pt/TiO_2-LTR	−0.9	0.2

hydrogenation at 373 K, 20 atm H_2 and 1 M citral in hexane, geraniol hydrogenation to citronellol is negligible compared to citronellal hydrogenation to citronellol. Furthermore, hydrogenation of geraniol alone resulted in a high initial reaction rate followed by deactivation to a negligible rate [30]. With this information, hydrogenation of geraniol + nerol to citronellol was assumed to be kinetically insignificant during citral hydrogenation at 373 K and 20 atm H_2, i.e. reaction 3 in Fig. 1 is negligible under these conditions and citronellol is formed primarily via hydrogenation of citronellal. The low concentrations of citronellal in the bulk liquid phase during citral hydrogenation suggest that citronellal rapidly hydrogenates to citronellol. In addition, it can be concluded that the reaction rate for step 6 in Fig. 1 is also negligible since no 3,7-dimethyloctanol was detected. Finally, isomerization of the unsaturated alcohol to citronellal is assumed to be negligible because this was found experimentally with Pt/SiO_2 catalysts [30], and it is consistent with the suppression of the vapor-phase rate of crotyl alcohol isomerization to butyraldehyde observed with Pt/TiO_2-HTR compared to Pt/SiO_2 [5]. With these simplifications, the instantaneous selectivity to geraniol + nerol (UALC) can then be defined as follows:

$$S_{\mathrm{UALC}}^{\mathrm{INST}} = \frac{r_1}{r_1 + r_2 + r_4 + r_5} = \frac{\mathrm{d(Geraniol + nerol)}/\mathrm{d}t}{\mathrm{d(Geraniol + nerol)}/\mathrm{d}t + \mathrm{d(Citronellol)}/\mathrm{d}t + \mathrm{d(Isopulegol)}/\mathrm{d}t} \quad (3)$$

The instantaneous selectivity was evaluated by fitting the temporal concentration profiles (Figs. 3a and 6a) to a polynomial which was subsequently used to evaluate the derivatives. Fig. 14a and b display the instantaneous selectivity versus conversion profiles for each of the reaction steps in Fig. 1 during citral hydrogenation over Pt/SiO_2 and Pt/TiO_2-HTR. Because Pt/TiO_2-LTR exhibits selectivity behavior similar to that for Pt/TiO_2-HTR, only the results for Pt/TiO_2-HTR are displayed in Fig. 14.

The instantaneous selectivity profiles for Pt/SiO_2 contrast sharply with the corresponding cumulative selectivity versus conversion profiles shown earlier. The instantaneous selectivity to unsaturated alcohol increases rapidly from 45 at 6% citral conversion to 90 at 11% citral conversion, then decreases monotonically with further increases in conversion, whereas the cumulative selectivity to unsaturated alcohol increases with increasing conversion [27]. The initial increase in the instantaneous selectivity to the unsaturated alcohol, which is accompanied by a decrease in the instantaneous selectivity to citronellal, occurs during the first 2 min of reaction where there is a rapid drop in hydrogen pressure inside the reactor (Fig. 13). Similar behavior has been observed earlier and it was speculated to be due to a surface modification, the details of which are not well understood, resulting in enhanced coordination and activation of the C=O bond to yield the unsaturated alcohol [27,36]. After this initial behavior, the rates of citronellal formation (r_2) and disappearance (r_4) increase simultaneously, resulting in a decrease in the net rate of formation of the unsaturated alcohol relative to that for formation of citronellol. The incremental selectivity profiles suggest that a non-deactivated Pt/SiO_2 catalyst more selectively hydrogenates the C=C bond, but surface modifications in the early stages of the reaction results in greater activation of the C=O bond. Furthermore, after the initial period, products due to hydrogenation of the C=C bond are accompanied by simultaneous hydrogenation of the C=O bond to yield citronellol. These arguments can also be extended to the Pt/TiO_2 catalysts, which exhibit a high initial selectivity for unsaturated alcohol. At higher conversions, citronellal formation is enhanced as is its rate of disappearance to yield citronellol, which results in an increase in the instantaneous selectivity to citronellol. The difference in the instantaneous selectivity versus conversion profiles between Pt/SiO_2 and Pt/TiO_2 is not as significant as evidenced earlier for vapor-phase benzaldehyde hydrogenation on Pt powder and TiO_2-promoted Pt powder [37].

The higher selectivity for hydrogenation of the C=O bond for analogous reactions over Pt/TiO_2-HTR catalysts has been attributed to oxygen vacancy sites on titania at the metal–support interface which interact with the lone pair of electrons on the carbonyl oxygen [13]. It is tempting to invoke similar arguments for the present work, but the similar selectivity vs. conversion behavior for Pt/TiO_2-LTR and Pt/TiO_2-HTR makes this difficult. Despite the large differences in

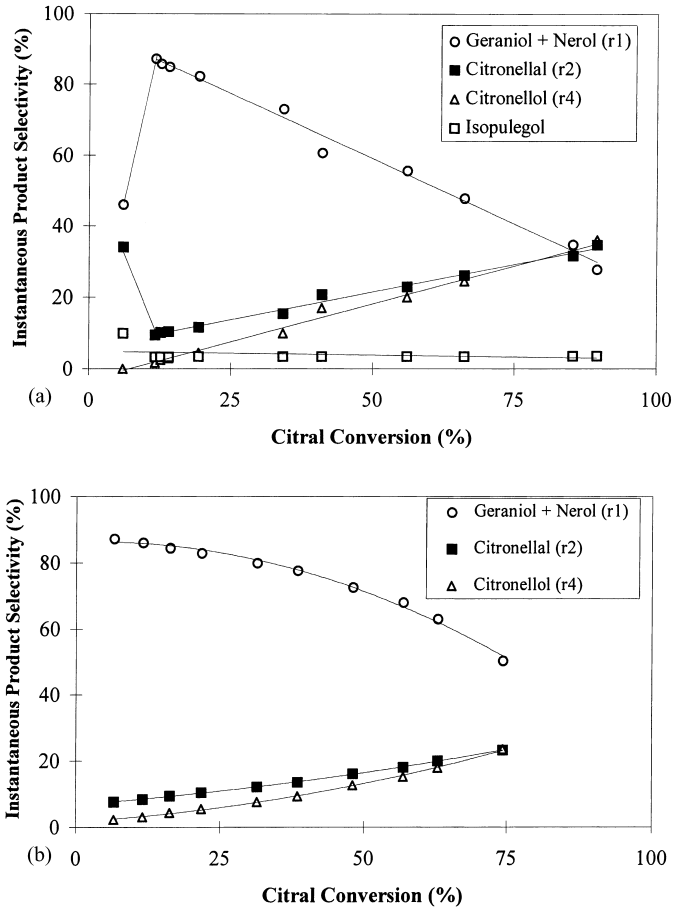

Fig. 14. Instantaneous selectivity to the unsaturated alcohol for (a)1.44% Pt/SiO_2 and (b) 1.78% Pt/TiO_2-HTR catalysts at 373 K, 20 atm H_2 and 1 M citral in hexane.

reaction rate (Fig. 8) and reaction orders (Table 3) among Pt/TiO_2-HTR, Pt/TiO_2-LTR and Pt/SiO_2, the instantaneous selectivity versus conversion behavior exhibited by the three catalysts is similar. This may be explained by the fact that reaction at higher temperatures enhances selectivity for hydrogenation of the C=O bond compared to the C=C bond. This is also seen in Fig. 12 that shows selectivity to the unsaturated alcohol increased over Pt/SiO_2 and Pt/TiO_2-LTR catalysts when the temperature increased from 298 to 373 K. The behavior was rationalized previously by comparing the respective bond dissociation energies of C=O and C=C bonds and the heats of adsorption for coordination via the C=C bond and C=O bonds. The C=O bond possesses a larger bond dissociation energy by 33 kcal/mol, thus its activation is more favored at higher reaction temperatures. Furthermore, the heat of adsorption of the carbonyl functionality is greater than that for the C=C bond, therefore, from a qualitative perspective, reaction at higher temperatures may result in greater coordination via the C=O bond as opposed to C=C bond [30]. Hydrogenation of the C=O bond on Pt would then be favored at higher reaction temperature and, as a result, the influence of MSI on product distribution is not as significant in the present system as it is during vapor-phase hydrogenation of crotonaldehyde, acetone and benzaldehyde [5,16,37].

In contrast to the behavior of Pt/SiO_2 and Pt/TiO_2-LTR, Pt/TiO_2-HTR exhibits conventional Arrhenius behavior between 298 and 403 K with an

activation barrier of 18 kcal/mol. The absence of an activity minimum with Pt/TiO_2-HTR is attributed to the influence of MSI on reaction kinetics. The higher activity at 373 K and standard conditions for Pt/TiO_2-HTR compared to Pt/TiO_2-LTR, i.e. a greater than threefold enhancement in rate (per gram catalyst) and a 50-fold enhancement in TOF, is attributed to the suppression of the decarbonylation reaction after the HTR pretreatment and the creation of new active sites at the metal–support interface which selectively hydrogenate the carbonyl bond.

DRIFTS spectra obtained during crotonaldehyde hydrogenation over TiO_2-supported Pt have shown significant suppression of any decarbonylation reaction after a HTR pretreatment [38]. This is consistent with the earlier discussion of hydrogenation over Pt/SiO_2 and Pt/TiO_2-LTR in which it was proposed that the lower initial rate at 373 K compared to that at 298 K was due to a greater fraction of the active sites covered by CO at 373 K. Suppression of decarbonylation reactions results in a greater fraction of sites available for hydrogenation. Decomposition of the alcohol to produce CO, which is proposed to occur over these catalysts, was shown by Shekhar and Barteau to be structure sensitive on Pd single crystal surfaces [39,40], and it has been well established that structure-sensitive reactions are inhibited by catalysts in the SMSI state [35]. The enhanced rate at 373 K is also due to the creation of oxygen vacancies and coordinatively unsaturated titania Ti^{2+} and Ti^{3+} cations at the metal–support interface which can interact with the lone pair electrons on the carbonyl oxygen thus activating the C=O bond. The concentration of these interfacial sites is significantly greater after HTR compared to LTR [11], and this results in a higher TOF for the HTR catalyst in spite of the 90% reduction in hydrogen and CO chemisorption. In the context of these two factors, the rate enhancement at 373 K is understandable. At 298 K, Pt/TiO_2-HTR exhibits a lower rate compared to Pt/SiO_2 and Pt/TiO_2-LTR because of the higher apparent activation energy exhibited by the Pt/TiO_2-HTR catalyst.

A support effect on citral hydrogenation was also manifested in the reaction orders with respect to the *E*- and *Z*-isomers of citral. Fig. 6 shows the temporal concentration profile for citral hydrogenation over 1.44% Pt/SiO_2, and the linear trendline drawn through the concentration profiles of the *E*- and *Z*-isomers indicates zero-order kinetics with respect to the concentration of each isomers. Furthermore, the TOF for disappearance of the *E*-isomer was approximately 1.5 times that for the *Z*-isomer. In contrast, the Pt/TiO_2-LTR and HTR catalysts exhibited near zero- and near first-order kinetics for the *Z*- and *E*-isomers, respectively, and the TOF for disappearance of the *E*-isomer was three to four times greater than that for the *Z*-isomer (Figs. 5 and 6b). Such a behavior cannot be attributed to an MSI effect since similar behavior is observed for both LTR and HTR catalysts. In addition, we can discount the role of *trans* to *cis* isomerization, which is thermodynamically feasible [41] and has been reported in the literature [42–44], because the rates of disappearance of *E*-citral and *Z*-citral are equal to the respective rates of formation of geranial and nerol, thus indicating that isomerization of *E*-citral (geranial) to *Z*-citral (neral) is not observed under reaction conditions. It is difficult to rationalize the higher reactivity of the *E*-isomer compared to the *Z*-isomer over TiO_2-supported catalysts; however this difference has possible application for kinetic separation of the *E*- and *Z*-isomers.

This type of isomerization reaction over metals is not well understood. Sheppard and coworkers reported *cis–trans* isomerization of 2-butenes over Pt/SiO_2 but found no evidence for this reaction over a Pt (1 1 1) surface, and they suggested that this was due to isomerization taking place on kink and edge sites present on Pt/SiO_2 catalysts but absent on a Pt (1 1 1) surface [43]. Alternatively, their results may indicate that the isomerization reaction observed on Pt/SiO_2 catalysts was catalyzed by hydroxyl groups on the SiO_2 rather than by Pt [42]. Somorjai and coworkers studied hydrogenation and isomerization of butenes and proposed that *cis–trans* isomerization of 2-butenes occurs via a 2-butyne surface intermediate. They suggested that *cis*-2-butene isomerizes via a dehydrogenation step to yield 2-butyne which is subsequently rehydrogenated to yield *trans*-2-butene [44]. The presence of hydrogen appears to be important for the isomerization of *cis*-citral to *trans*-citral. A Pt/TiO_2-HTR catalyst was purged with helium at 773 K after reduction, cooled in helium to 373 K, and 1 M citral in hexane under 20 atm He was added. No conversion, including isomerization of *trans*-citral to *cis*-citral, was obtained [28]. The greater reactivity for isomerization of *trans* to *cis* isomer during citral hydrogenation and the differences in reaction orders for the two isomers between the TiO_2-

and SiO_2-supported catalysts is not well understood, but in the context of the above discussion, it may be occurring on the support, at least partially.

The influence of MSI on citral hydrogenation kinetics is also observed in the reactant reaction orders, which were determined from initial rates at 373 K and summarized in Table 3. These values cannot be compared to those for other liquid-phase hydrogenation reactions because of the lack of such data. The order of 0.2 in hydrogen pressure observed for Pt/TiO_2-HTR is significantly different from the first-order dependence for Pt/SiO_2 and Pt/TiO_2-LTR. Similarly, the negative first-order dependency on citral concentration for Pt/TiO_2-HTR is distinctly different from the near zero-order dependence for Pt/SiO_2 and Pt/TiO_2-LTR catalysts. Both observations can be rationalized by a competitive adsorption model involving hydrogen and citral.

The reaction kinetics over a Pt/TiO_2-HTR catalyst were modeled using a conventional Langmuir–Hinshelwood model to correlate the initial rates as well as the rates of H_2 consumption at higher conversions, and they involved only two hydrogenation reactions, i.e. citral hydrogenation to either citronellal or to the unsaturated alcohol (geraniol + nerol). This is justifiable because the total selectivity to the unsaturated alcohol and citronellal is greater than 90% (Fig. 9). Moreover, the temporal H_2 consumption profile in Fig. 3b for citral hydrogenation at 373 K and standard conditions was compared to that calculated from the concentration data assuming citral hydrogenation only to citronellal and the unsaturated alcohol, and the results agree well. The reaction model is shown by the following sequence of elementary steps.

$$H_2 + 2S \overset{K_H}{\rightleftharpoons} 2H\text{–}S \tag{4a}$$

$$Cit + S \overset{K_{Cit}}{\rightleftharpoons} Cit\text{–}S \tag{4b}$$

$$Cit\text{–}S + H\text{–}S \overset{k_i}{\rightarrow} HCit\text{–}S + S \tag{4c}$$

$$HCit\text{–}S + H\text{–}S \overset{1/K_P}{\rightleftharpoons} Product + 2S \tag{4d}$$

Quasi-equilibrium was assumed for adsorption of hydrogen and citral (Cit) on a single type of site, S. The surface coverages of citral and hydrogen can then be represented as

$$\Theta_{Cit} = K_{Cit} C_{Cit} \Theta_S \tag{5a}$$

$$\Theta_H = K_H^{1/2} P_H^{1/2} \Theta_S \tag{5b}$$

where K_i and Θ_i are the adsorption equilibrium constants and fractional surface coverage of species i, respectively. The rate expression then becomes

$$r = k_i \Theta_{Cit} \Theta_H = L k_i K_{Cit} K_H^{1/2} C_{Cit} P_H^{1/2} \Theta_S^2 \tag{6}$$

where L is the total number of active sites. This rate expression is applicable to the formation of unsaturated alcohol (geraniol + nerol) with a rate constant k_1 and citronellal with a rate constant k_2, with k_1 assumed to be the average rate constant for geraniol and nerol formation. No effort was made to distinguish between the reactivity of the two isomers. The expression for Θ_s can be obtained only after including a sequence of inhibiting decomposition reactions, consistent with an earlier proposal [27] for reasons that will be addressed subsequently, which is described as follows:

$$UALC\text{–}S + S \overset{K_{ET}}{\rightleftharpoons} Etoxy\text{–}S + H\text{–}S \tag{7a}$$

$$Etoxy\text{–}S + 2S \overset{K_{ACT}}{\rightleftharpoons} Acyl\text{–}S + 2H\text{–}S \tag{7b}$$

$$Acyl\text{–}S + S \overset{k_{ACT}}{\rightarrow} CO\text{–}S + C'S\text{–} \tag{7c}$$

$$CO\text{–}S \overset{k_D}{\rightarrow} CO + S \tag{7d}$$

$$C'\text{–}S + H\text{–}S \overset{k_{HC}}{\rightarrow} H_2C' + 2S \tag{7e}$$

where Etoxy–S, Acyl–S, and C′–S represent adsorbed ethoxy, acyl-type, and carbonaceous species, respectively arising from the decarbonylation reaction. Assuming only citral, H atoms, and CO exist as significant surface species, the site balance is

$$\Theta_{Cit} + \Theta_H + \Theta_S + \Theta_{CO} = 1 \quad \text{and} \tag{8a}$$

$$\Theta_S = \frac{1 - \Theta_{CO}}{1 + K_{Cit} C_{Cit} + K_H^{1/2} P_H^{1/2}} \tag{8b}$$

where Θ_{CO} represents the fractional surface coverage of CO represented by the difference between the rate of the decomposition reaction and the desorption of CO and described by Eqs. (7a)–(7d). The change in CO coverage with time is

$$\frac{d\Theta_{CO}}{dt} = L K_{ACT} \Theta_{ACYL} \Theta_S - L k_D \Theta_{CO} \tag{9}$$

which after appropriate substitutions based on

Eqs. (7a) and (7b) becomes

$$\frac{d\Theta_{CO}}{dt} = LK_{ET}K_{ACT}k_{ACT}K_{UALC}K_H^{-3/2}C_{UALC}P_H^{-3/2} \times \Theta_S^2 - Lk_D\Theta_{CO} = k'_{CO}C_{UALC}\Theta_S^2 - k_D\Theta_{CO} \quad (10)$$

where k'_{CO} and k_D are the apparent rate constants for the decarbonylation reaction and CO desorption, respectively. The rate expression for hydrogenation then is

$$r = \frac{kK_{Cit}K_H^{1/2}C_{Cit}P_H^{1/2}}{(1 + K_{Cit}C_{Cit} + K_H^{1/2}P_H^{1/2})^2}(1 - \Theta_{CO})^2 \quad (11)$$

where $k = L(k_1 + k_2)$. This rate expression is coupled with Eq. (10), with k, K_{Cit}, K_H, and k'_{CO} as adjustable parameters.

For the purpose of modeling the initial rates, it was assumed that the surface coverage of CO was negligible, thus yielding the following simplified expression for the initial rate of citral disappearance:

$$r = \frac{kK_{Cit}K_H^{1/2}C_{Cit}P_H^{1/2}}{(1 + K_{Cit}C_{Cit} + K_H^{1/2}P_H^{1/2})^2} \quad (12)$$

This expression correlated the experimental data well and the fits are shown in Fig. 15 for reaction at 343, 373 and 403 K for citral concentrations of 0.5–6.0 M in hexane and H_2 pressures from 7 to 41 atm. Optimum parameters were determined using the Solver Routine in Microsoft Excel and a nonlinear regression package from Micromath Scientific Software (Scientist). The optimal parameters are tabulated in Table 5 based on a standard state of 1 atm in the gas phase for the enthalpy and entropy of adsorption values using a procedure outlined previously [26,45]. The enthalpy of adsorption is negative as expected from thermodynamics [45,46], and the value of −26 kcal/mol

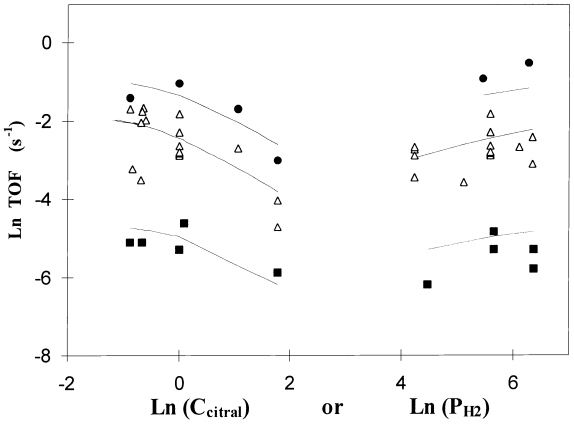

Fig. 15. Fit of kinetic model (Eq. (12)) to the initial turnover frequency for citral disappearance between 343 K (■), 373 K (△) and 403 K (●), 7–41 atm H_2, and 0.5–6.0 M citral in hexane.

obtained for citral is similar to that for Pt/SiO_2 catalysts [27]. The enthalpy of adsorption for hydrogen was −21 kcal/mol, which is in good agreement with the value of 19 kcal/mol reported for the initial hydrogen heat of adsorption [47] and values of 13–19 kcal/mol for integral heats of adsorption [48] on Pt/TiO_2-HTR catalysts. The respective entropies of adsorption for citral and hydrogen were −42 and −27 e.u., and these entropy losses are below the respective standard entropies in the gas phase at 298 K, which are 83 and 31 e.u. [28,41], as required [45,46].

As mentioned previously, the reaction rate in terms of H_2 consumption was monitored up to 80% conversion; therefore, the model proposed above was extended to test its predictive capabilities at higher conversions and in the presence of CO from the decomposition reaction. The values of the rate constants and the adsorption equilibrium constants for fitting H_2 uptakes at higher conversions were those in Table 5 obtained from the initial rates. A value for k_1, i.e. the

Table 5
Fitting parameters obtained from non-linear regression of initial rate and H_2 uptakes (Eqs. (9) and (10))

	343 K	373 K	403 K	E_a or ΔH^0_{ad}	ln (A_o) or S^0_{ad}
$k_1 + k_2$ (h^{-1})	417676	729837	97888	18	22
K_{cit} (l/mol)	13965	7066	1917	−26	−42
K_H (atm^{-1})	97823	10353	1500	−19	−27
k'_{CO} (mol/h)	4.20E+10	1.40E+13	7.30E+12	–	–
k_D[a] (h^{-1})	0.96	20.5	281	26	30

[a] Obtained from McCabe and Schmidt [49].

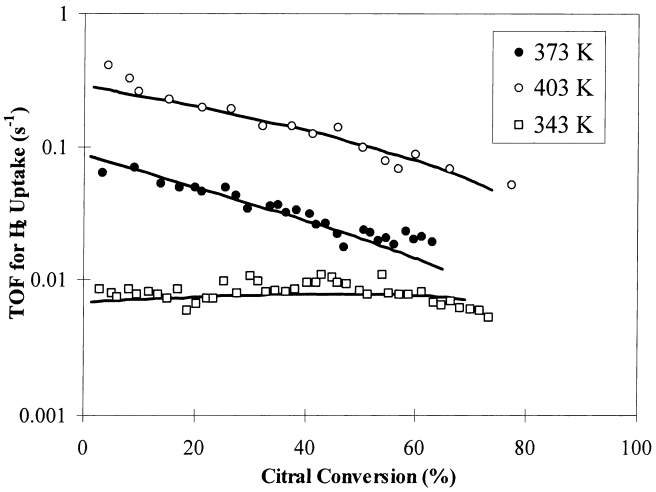

Fig. 16. Fit of kinetic model (Eqs. (10)–(12)) to the turnover frequency for H_2 uptake during citral hydrogenation at 343 K (□), 373 K (●) and 403 K (○) with 1 M citral in hexane at 20 atm H_2.

rate constant for formation of unsaturated alcohol, was acquired by assuming that $k_1 = 0.9(k_1 + k_2)$ because the selectivity to the unsaturated alcohol was 90% during the initial stages of the reaction. It is important to include a deactivation step because its exclusion results in a model with citral concentration to the first order in the numerator and citral concentration to the second order in the denominator. Furthermore, when the values listed in Table 5 are used in Eq. (12) without the decomposition reactions, the model yields an increasing reaction rate with increasing citral conversion, which is inconsistent with that reported in Fig. 3b where the rate of H_2 uptake decreases with increasing citral conversion. Inclusion of the unsaturated alcohol decomposition reaction necessitates only one additional fitting parameter, namely the apparent rate constant for the decarbonylation reaction, i.e. k'_{CO}. All additional parameters including k_1, $k_1 + k_2$, K_{Cit}, K_H were constrained to those based on parameter estimation using the initial rates, and the rate constant for CO desorption, k_D, was based on the work of McCabe and Schmidt reporting an activation energy and pre-exponential factor of 26 kcal/mol and 10^{13} s^{-1}, respectively, for CO desorption from a Pt (1 1 1) surface [49]. Figs. 15 and 16 displays the fit of the kinetic model with the deactivation steps included (Eq. (10)) to the experimental data for 343, 373, and 403 K at standard conditions. The apparent rate constants for the decarbonylation reaction and CO desorption are also listed in Table 5.

It should be noted that the details of the geraniol and nerol decomposition reaction are not well understood and the mechanism assumed in Eqs. (7a)–(7e) was based on detailed spectroscopic studies of Barteau and coworkers for similar systems over single crystal Pd surfaces [39,40]. It is unclear whether decomposition of the unsaturated alcohol over Pt proceeds via an acyl intermediate, as proposed for Pd surfaces [39,40], or via η^3-type alkoxide [50] or oxametallocycle [51] species proposed for Rh surfaces for unsaturated and saturated alcohols, respectively. Regardless, it is our assertion that this decomposition reaction plays an important role in the kinetics of citral hydrogenation over SiO_2- and TiO_2-supported Pt catalysts.

5. Summary

Liquid-phase hydrogenation of citral was studied at concentrations of 0.5–5.9 M citral in hexane between 298 and 403 K and 7 to 41 atm H_2. Pt/TiO_2-HTR catalysts exhibit a 50-fold enhancement in the initial TOF for citral disappearance compared to Pt/TiO_2-LTR and a 100-fold increase in TOF compared to Pt/SiO_2 catalysts. The reaction kinetics with Pt/TiO_2-LTR were similar to those reported earlier for Pt/SiO_2 cat-

alysts, and they exhibited an activity minimum with respect to temperature, a near zero-order dependence on citral concentration, and a first-order dependence on hydrogen pressure. In contrast, Pt/TiO_2-HTR exhibited conventional Arrhenius behavior, a negative first-order dependence on citral concentration, and a near zero-order dependence on H_2 pressure. The reaction on Pt/TiO_2-HTR was modeled by a conventional Langmuir–Hinshelwood expression invoking one type of site and the addition of the first H atom as the rate determining step. In addition, a sequence of steps describing decomposition of the unsaturated alcohol to produce CO was invoked to explain the deactivation behavior. This explanation had previously been used successfully for Pt/SiO_2 catalysts. The model described the reaction kinetics well and generated thermodynamically consistent parameters. In summary, MSI can affect not only reaction rates, but also kinetic parameters in the rate expression, and deactivation processes can be inhibited.

Acknowledgements

This study was supported by the DOE, Division of Basic Energy Sciences under Grant No. DE-FE02-84ER13276.

References

[1] P. Gallezot, D. Richard, Catal. Rev. Sci. Eng. 40 (1998) 81.
[2] P. Claus, Top. Catal. 5 (1998) 51.
[3] M. Ash, I. Ash, Specialty Chemicals Source Book, 1st Edition, Synapse Information Resources Inc., New York, 1997.
[4] R. Touroude, J. Catal. 65 (1980) 110.
[5] B. Sen, M.A. Vannice, J. Catal. 115 (1989) 65.
[6] T.B.L.W. Marinelli, S. Nabuurs, V. Ponec, J. Catal. 151 (1995) 431.
[7] H. Yoshitake, K. Asakura, Y. Iwasawa, J. Chem. Soc., Faraday Trans. 85 (1989) 2021.
[8] L. Mercadante, G. Neri, C. Milone, A. Donato, S. Galvagno, J. Mol. Catal. A: Chem. 105 (1996) 93.
[9] G. Neri, L. Mercadante, C. Milone, R. Pietropaolo, S. Galvagno, J. Mol. Catal A: Chem. 108 (1996) 41.
[10] S.J. Tauster, S.C. Fung, R.L. Garten, J. Am. Chem. Soc. 100 (1978) 170.
[11] G.L. Haller, D.E. Resasco, Adv. Catal. 36 (1989) 173.
[12] S.A. Stevenson, J.A. Dumesic, R.T.K. Baker, E. Ruckenstein, Metal support interactions, in: Catalysis, Sintering, and Redispersion, Van Nostrand Reinhold, New York, 1987.
[13] M.A. Vannice, Catal. Today 12 (1992) 255.
[14] M.A. Vannice, Top. Catal. 4 (1997) 241.
[15] C.S. Ko, R.J. Gorte, Surf. Sci. 155 (1985) 296.
[16] B. Sen, M.A. Vannice, J. Catal. 113 (1988) 52.
[17] H. Yoshitake, Y. Iwasawa, J. Catal. 125 (1990) 227.
[18] B. Coq, P.S. Kumbhar, P. Moreau, F. Figueras, J. Phys. Chem. 98 (1994) 10180.
[19] A.A. Wismeijer, A.P.G. Kieboom, H. VanBekkum, Appl. Catal. 25 (1996) 181.
[20] M. Englisch, A. Jentys, J.A. Lercher, J. Catal. 166 (1997) 25.
[21] Y. Nagase, H. Nakamura, Y. Yazawa, T. Imamoto, Nippon Kagaku Kaishi 9 (1992) 922.
[22] R.J. Madon, M. Boudart, Ind. Eng. Chem. Fundam. 21 (1982) 438.
[23] H.S. Fogler, Elements of Chemical Reaction Engineering, 2nd Edition, Prentice Hall, Englewood, NJ, 1992, p. 625.
[24] J.B.F. Anderson, R. Burch, Appl. Catal. 25 (1986) 173.
[25] M.B. Palmer, M.A. Vannice, J. Chem. Tech. Biotechnol. 30 (1980) 205.
[26] U.K. Singh, M.A. Vannice, AIChE J. 45 (1999) 1059.
[27] U.K. Singh, M.A. Vannice J. Catalysis 191 (2000) 165.
[28] U.K. Singh, Ph.D. Thesis, Pennsylvania State University, 2000.
[29] R.T.K. Baker, E.B. Prestridge, R.L. Garten, J. Catal. 59 (1979) 293.
[30] U.K. Singh, M.N. Sysak, M.A. Vannice, J. Catalysis 191 (2000) 181.
[31] M.J. Masson, M.S. Thesis, Pennsylvania State University, in preparation.
[32] U.K. Singh, M.A. Vannice, 12th International Congress on Catalysis, Stud. Surf. Sci. & Catal. 130 (2000) 487.
[33] M. Boudart, Adv. Catal. 20 (1969) 153.
[34] J.J. Carberry, in: Chemical and Catalytic Engineering, McGraw-Hill, NewYork, 1976. (Chapter 5)
[35] D.E. Resasco, G.L. Haller, J. Catal. 82 (1983) 279.
[36] P. Gallezot, A. Giroir-Fendler, D. Richard, in: W.E. Pascoe (Ed.), Chemical Industry 47, Catalysis of Organic Reactions, 1992.
[37] M.A. Vannice, D.J. Poondi, J. Catalysis 178 (1998) 386.
[38] A. Dandekar, M.A. Vannice, J. Catal. 183 (1999) 344.
[39] R. Shekhar, M. Barteau, Catal. Lett. 31 (1995) 221.
[40] R. Shekhar, M. Barteau, Surf. Sci. 319 (1994) 298.
[41] R.C. Reid, J.M. Prausnitz, T.K. Sherwood, The Properties of Gases and Liquids, McGraw-Hill,New York, 1977.
[42] M. Englisch, V.S. Ranade, J.A. Lercher, Appl. Catal. A: Gen 163 (1997) 111.
[43] M.A. Chesters, C. De La Cruz, P. Gardner, E.M. McCash, P. Pudney, G. Shahid, N. Sheppard, J. Chem. Soc., Faraday Trans. 86 (1990) 2757.
[44] C. Yoon, M.X. Yang, G.A. Somorjai, J. Catal. 176 (1998) 35.
[45] M.A. Vannice, S.H. Hyun, B. Kalpakci, W.C. Liauh, J. Catal. 56 (1979) 358.
[46] M. Boudart, AIChE J. 18 (1972) 465.
[47] J.M. Herrmann, M. Gravelle-Rameau-Maillot, P.C. Gravelle, J. Catal. 104 136.
[48] B. Sen, P. Chou, M.A. Vannice, J. Catal. 101 (1986) 517.
[49] R.W. McCabe, L.D. Schmidt, Surf. Sci. 66 (1977) 101.
[50] N.F. Brown, M.A. Barteau, J. Am. Chem. Soc. 114 (1992) 4258.
[51] C.J. Houtman, M.A. Barteau, J. Catal. 130 (1991) 528.